

Removal of slightly heavy gases from a valley by crosswinds

Ian P. Castro^{a,*}, Ajay Kumar^b, William H. Snyder^{c,**} and S. Pal S. Arya^d

^a Department of Mechanical Engineering, University of Surrey, Guildford, GU2 5XH (England)

^b Sirmine Environmental Consultants, Cary, NC 27511 (USA)

^c Atmospheric Sciences Modeling Division, National Oceanic and Atmospheric Administration, Research Triangle Park, NC 27711 (USA)

^d Department of Marine, Earth and Atmospheric Sciences, North Carolina State University, Raleigh, NC 27612 (USA)

(Received September 17, 1992; accepted in revised form February 19, 1993)

Abstract

Wind tunnel experiments made to determine how rapidly dense gas is removed from a topographical depression by a crosswind are reported. The density and flow rate of the gas (input at the bottom of a V-shaped valley in otherwise homogeneous, flat terrain) were together sufficiently low to prevent pooling of the gas on the valley floor. In terms of the earlier and complimentary work of Briggs et al. (*J. Hazardous Mater.*, 24 (1990) 1–33), who considered only pooling cases, the present work concentrates on cases for which the relevant Richardson numbers ($Ri_0 = gH\Delta\rho/(\rho U_0^2)$) are relatively low. A simple theory is described, based on assumptions about the way in which the (slightly) heavy gas is removed by turbulent entrainment from the separated flow in the valley. For the steady state case, the theoretical result $C_0/C_s = \varepsilon V_0 (1 + \alpha Ri_0^n)$ is shown to fit the data quite well, where C_0/C_s is the ratio of the average valley concentration to the source gas concentration, V_0 is the dimensionless source flow rate and ε , α and n are constants. For the transient experiments, in which the source was suddenly removed and the decay of valley concentration was measured, the data are shown to be reasonably consistent with the theory, for both neutral and heavy gas releases: $-\ln(C') + \alpha Ri_0^n (1 - C'^n)/n = t'/\tau$, where $C' = C(t)/C_s$ and τ is a decay time constant. Although Reynolds number effects are shown to be significant in certain cases, the results provide a framework for estimating how long a heavy gas spill will take to disperse from depressions which are sufficiently steep-sided to embody regions of separation in windy conditions aloft.

*To whom correspondence should be addressed.

**On assignment to the Atmospheric Research and Exposure Assessment Laboratory, US Environmental Protection Agency, Research Triangle Park, NC 27711 (USA).

1. Introduction

Many of the accidental releases of toxic chemicals into the atmosphere or oceans involve material that is denser than the environment. The dispersion of such releases is consequently dependent, in part, on fluid dynamical parameters involving the density difference. In general, the rate of dispersion measured at, say, a specific location downwind of the release will be reduced as this density difference increases and this will be particularly true if the release occurs in a topographical depression. In the latter case it is clear that more energy will be required to extract the material from the depression than in the case of a neutrally stable release — simply because the potential energy gain required of the dense material is greater than it would otherwise be.

If enough dense material is released sufficiently quickly, it may actually collect at the bottom of the depression, decouple from the wind aloft and form a 'pool' of some vertical thickness before it is entrained and thence removed by a crosswind. The initial entrainment process is then dominated by the nature of the interface between the pool and the region above it. There is a considerable literature on the general problem of mixing between a lighter fluid moving over a heavier one (see, for example, the review by Christodoulou [2]). Recently, Briggs et al. [1] (hereafter BTS) have also conducted a series of experiments whose purpose was to determine how rapidly dense gas trapped in a valley could be removed by a crosswind. Their experiments concentrated on cases in which pooling of dense gas occurred and the entrainment was therefore 'interface dominated'. They undertook both steady experiments, in which the pool height remained fixed because of a balance between the heavy gas emission rate at the valley bottom and the entrainment rate across the interface, and transient experiments, in which effectively the source was removed and the pool height then decreased with time. These latter experiments were shown to confirm predictions based on the steady-state results.

BTS did not address the question of how the dispersion rate changes under conditions where there is no pool. They found that, in the transient experiments, once the pool height had reduced to zero there was a sudden increase in the rate of removal of gas from the valley, but the experiments were not designed to study this latter phase of the dispersion process. This increased removal rate was almost certainly caused by the fact that there was no longer a clearly distinguishable interface between heavy and light fluids so that entrainment from the valley was then dominated by the rate at which fluid could be removed from the top of the recirculating flow region (which largely filled the valley), rather than the rate at which it could be fed into the bottom of the recirculating region via entrainment across a density interface. It is this 'slightly dense' gas dispersion process that is addressed in this paper. We consider only cases in which there is no dense gas pool, so that the concentration of heavy gas is everywhere significantly less than the source value. In practice, this could arise in cases of small gas releases, releases of slightly dense material, releases in relatively windy conditions, or some combination of

these. Despite the lack of a pool, one still expects reductions in the dispersion rate (compared with the neutral case); from a practical perspective, the problem is likely to be equally important, particularly for more toxic releases, when even very small concentrations can be extremely hazardous.

The practical problem is always likely to be most severe when the geometry is such that the release is contained in or near a recirculating region of flow. This is most common in the context of releases near buildings and the question of how long removal takes from a recirculating building wake has been addressed previously, for the case of neutral releases (e.g. Hunt and Castro [3]). It was found in that case that the rate of decay of neutrally-buoyant emissions from within the wake could be described solely in terms of the geometrical size of the recirculating region and a typical upstream velocity; it was largely independent of the presence of strong mean swirling motions generated by some building shapes and orientations. This is in contrast to the behaviour well downstream of the recirculating wake, where concentration levels can depend crucially on such motions (as shown by, for example, Peterka and Cermak [4] in the context of buildings and Castro and Snyder [5] in the context of hills). To our knowledge no work has been done on the corresponding cases when the effluent is heavier than air.

In the experiments described in this paper we retain the simple geometrical features of the V-shaped valley used by BTS, recognising that this might be in some respects a 'worst case' topographical situation because of the recirculation which exists in the valley (although even worse cases might be those associated with perpendicular-sided valleys, like street canyons). The work is therefore an extension of the earlier experiment — indeed, the measurements were undertaken in the same wind tunnel and many features of the experimental procedure were identical. In the following section some simple theoretical ideas are described. These take as their basis ideas originally discussed by Humphries and Vincent [6] and later applied by Vincent [7], Hunt and Castro [3] and Fackrell [8] in the context of dispersion of passive materials in building wakes. Relationships are derived governing both the steady-state concentration at a typical location within the valley in terms of source flow rate and Richardson number, and the rate at which the concentration falls when the source is removed. The experimental procedures are summarised in Section 3 and Section 4 presents and discusses the major results. Conclusions and a typical application of the results are given in the final section.

2. Theoretical considerations

Figure 1 is a sketch of the flow geometry considered in this paper. A valley of width W (in the flow direction), length L (in the spanwise direction) and depth H is located in an otherwise homogeneous terrain across which there is an ambient wind $U(z)$. We assume throughout this work that L/W is sufficiently large that the flow can for practical purposes be considered two-dimensional;

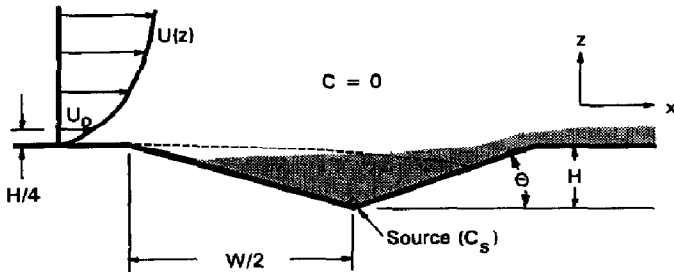


Fig. 1. Valley cross-section, definition sketch. Dotted line is postulated separation-reattachment streamline in (2D) neutral flow.

measurements (see Section 3) showed that even for L/W of only about 1.4, variations in mean concentration along a lateral line within the separation region varied by less than 10% within the central two-thirds of the span. Provided $H \gg z_0$, the roughness length of the upstream surface, the dynamics of the flow within the valley will not depend critically on z_0 and, if the valley sides are sufficiently steep, flow separation will occur near the upstream edge and the valley flow will be dominated by a large recirculation region. We imagine a source of gas at the bottom of the valley and therefore well within the recirculating flow. If the average volumetric concentration of the gas in the valley is C_0 , then the volumetric flux, F , out of the valley will, on dimensional grounds, be given by:

$$F = k_1 A U_c C_0 \quad (1)$$

where k_1 is a constant and A is the area across which fluid is being entrained out of the valley at some average entrainment velocity, U_c . This argument is valid whether the flux is caused by turbulent transport or by direct advection or a mixture of the two processes. The constant k_1 represents the fact that the gas being extracted from the valley by entrainment will in general not have the same concentration as the valley-averaged value.

For a source of gas of concentration C_s and volumetric flow rate V_s /unit length, steady-state conditions require:

$$F = L V_s C_s = k_1 A U_c C_0, \quad (2)$$

where L is the valley cross-stream length, so that the steady state valley concentration can be expressed as:

$$C_0/C_s = (V_s/HU_c)/k_1 k_2, \quad (3)$$

in which the entrainment area, A , has been replaced by $k_2 HL$ (with k_2 depending on valley geometry). If the source is suddenly removed, the rate of change of the total quantity of gas, of average concentration C , in the valley is given by:

$$-d(VC)/dt = F = k_1 A U_c C, \quad (4)$$

where V is the volume of the valley.

In the case of a neutral gas release, the average entrainment velocity can be assumed, on dimensional grounds, to be some constant fraction of a typical velocity in the upstream flow, U_0 , say (so that $U_e = k_3 U_0$). Then the steady-state concentration (C_0) is given from eq. (3) by:

$$C_0/C_s = V_0/(k_1 k_2 k_3), \quad (5)$$

where $V_0 = (V_s/HU_0)$ (and must clearly be less than $k_1 k_2 k_3$) and the variation of C with time after removal of the steady source is given from eq. (4) by:

$$-\ln(C/C_0) = (k_1 k_3/k_4)(tU_0/H), \quad (6)$$

in which the length scale, V/A , has been written as $k_4 H$, with, again, k_4 depending on valley geometry. C_0 is the initial value of C when the source is removed. (Note that eq. (5) can be written as $C_0 U_0 A/q = (k_1 k_2)^{-1} = \text{const.}$, with $q = C_s V_s L$, emphasising that for given source conditions and valley geometry, the steady concentration is inversely proportional to the upstream velocity.) Equation (6) suggests that the valley concentration will fall exponentially with time on removal of the source, at a non-dimensional rate dependent only on the constants, which depend on the particular valley geometry. In cases of neutral releases in recirculating building wakes, eq. (6) has been shown to describe the variation of wake concentration very well (e.g. Hunt and Castro [3]). There is no obvious reason why the above arguments should not hold equally well in the present case.

In the case of release of a (slightly) heavy gas, it is expected that the effective entrainment velocity, U_e , will depend on a Richardson number appropriate to the flow in the entrainment region. Assuming that this region can be characterised by some mixing layer of average thickness δ , a suitable Richardson number is given by $Ri = g(\Delta\rho/\rho_a)\delta/U_0^2$, where $\Delta\rho$ is an average density difference across the mixing region and ρ_a is the ambient air density. Recall that we are *not* considering the more extreme case in which there is a heavy gas pool, when the limiting entrainment process is at the pool interface, beneath the separated flow region. Here, we are assuming that the entrainment process is essentially the same as it is in the case of a neutral release, and therefore occurs largely in the mixing region just *above* the separated flow region but is somewhat damped by the nature of the density variation across the entrainment region. Density differences are related directly to gas concentrations and, assuming for the moment that the average valley concentration used earlier, C , can be taken as the value appropriate for the density ratio, Ri will be proportional to $(\gamma C_s g H/U_0^2)(\delta/H)(C/C_s)$, where γ is the factor relating the concentration to the density difference ($\gamma C_s = \Delta\rho_s/\rho_a$). A simple expression for the entrainment velocity might then be:

$$U_e/U_0 = k_3/\{1 + k_5[Ri_s(\delta/H)(C/C_s)]^n\}, \quad (7)$$

where $Ri_s = \gamma C_s g H/U_0^2$, a Richardson number appropriate to the source, and n and k_5 are constants. Note that $Ri_s = 1/Fr_0$, in the BTS terminology. Note also that with propane (or a propane/ CO_2 mixture) as the source gas, which was the

case for all the heavy gas experiments, $\gamma C_s = (44 - 29)/29 = 0.52$. Equation (7) reduces to the relation used in the neutral case if $Ri_s = 0$ and implies a monotonic reduction in U_e as Ri_s rises. Use of this expression in eq. (3) leads to the steady-state result:

$$C_0/C_s = V_0[1 + k_5(Ri_0\delta/H)^n]/k_1k_2k_3, \quad (8)$$

and, in eq. (4), to the transient result:

$$-\ln(C') + (k_5/n)(Ri_0\delta/H)^n(1 - C'^n) = (k_1k_3/k_4)t', \quad (9)$$

where $C' = C/C_0$, $t' = tU_0/H$ and $Ri_0 = Ri_s C_0/C_s$. Note that the arguments leading to these results for dense gas releases have ignored the possibility that some of the constants might, in fact, be functions of Ri . In deriving eq. (9) it has also been assumed that δ/H is constant with time.

With increasing Ri one would eventually expect some changes in the nature of the recirculating flow within the valley, which might lead to changes in k_1 , k_2 and k_4 as well as in the average entrainment layer thickness, δ . Figure 14, discussed more fully in Section 5, shows that the steady-state concentration pattern within the valley for conditions near pooling is rather different from that for a neutral release. However, our experimental data will be analysed in terms of the above results on the basis that such effects will only be of second order, provided conditions near the valley bottom are not too close to pooling conditions. Regrouping constants and assuming $(\delta/H)^n$ is another constant allows eqs. (8) and (9) to be rewritten as:

$$C_0/C_s = \varepsilon V_0(1 + \alpha Ri_0^n) \quad (10)$$

and

$$-\ln(C') + \alpha Ri_0^n(1 - C'^n)/n = t'/\tau, \quad (11)$$

respectively, where $\tau = k_4/(k_1k_3)$ (a non-dimensional time constant), $\varepsilon = 1/(k_1k_2k_3)$ and $\alpha = k_5(\delta/H)^n$. Neutral-release steady-state and transient experiments allow ε and τ , respectively, to be determined and heavy gas release experiments can then be used to see, first, whether steady-state conditions are modelled adequately by eq. (10) with appropriate values of α and n and then, second, whether or not (with the same constants) eq. (11) describes the transient behaviour. Equations (10) and (11) constitute the principal theoretical results of the present work.

Finally, it should be emphasised again that these results have all been obtained on the assumption that there is no heavy gas pooling in the valley. At a given windspeed, the source rate required to begin the pooling state will be a function only of Ri_s and, presumably, a Reynolds number — $Re_0 = U_0H/\nu$, say. In pooling cases, one of the implications of the data presented by BTS (who used the same valleys) is that for the limit of zero pool height,

$$V_0 Ri_s = c(1 + 0.46/Re_f), \quad (12)$$

where c is a constant (0.00048) and $Re_f = (H/W)V_0 Re_0 / Ri_s$. ($V_0 Ri_s = V'$ in the notation of BTS). Note that this is an extrapolation beyond the valid limit of the BTS data. Some initial experiments to determine the pooling criterion, in terms of the lowest tunnel speed required to prevent pool formation for a given source flow rate, will be compared with this result later. Note, however, that in the limit of zero wind speed, the above relationship fails, for it predicts that a pool will occur at *any* finite flow rate, whereas one expects that laminar diffusion will prevent a pool if the source rate is low enough. In that case, one could argue that, since vertical diffusion will occur across a layer of thickness d , say, pooling will begin when this thickness is such that the surface area (W' , per unit spanwise length) of the top of the diffusing layer is just insufficient to allow enough total diffusion ($W'\kappa C_s/d$, where κ is the molecular diffusivity) to balance the input source rate ($V_s C_s$). For the triangular valley of the present case, $2d/W' = \tan \theta$, where θ is the valley side-wall slope, so that pooling will begin when

$$V_s = V_p = 2\kappa/\tan \theta. \quad (13)$$

3. Experimental procedures

All experiments were conducted in the Meteorological Wind Tunnel of the EPA Fluid Modeling Facility, fully described by Snyder [9]. The valley models were sunk into the floor of the wind tunnel and had the dimensions given in Table 1, with most measurements made using the larger of the two models. They did not span the entire working section, but steady-state measurements of concentration along a lateral line within the separation region showed variations within $\pm 10\%$ over the central two-thirds of the span. Two-dimensionality was always better in cases of heavy gas releases. The boundary layer used for all experiments was identical with that used by BTS and was developed over a rough surface comprising a homogeneous layer of stones (commercially known as Sanspray) with a mean diameter of about 1 cm. A tripping fence, 15.3 cm in height, was located 65 cm downstream from the test section entrance. This configuration lead to velocity and turbulence profiles, shown in

TABLE 1

Dimensions of valley models

Valley	Length (m) (crosswind)	Width (m) (along wind)	Depth (m)	Wall slope ($^\circ$)
Large	2.0	1.4	0.254	20
Small	1.0	0.7	0.140	22

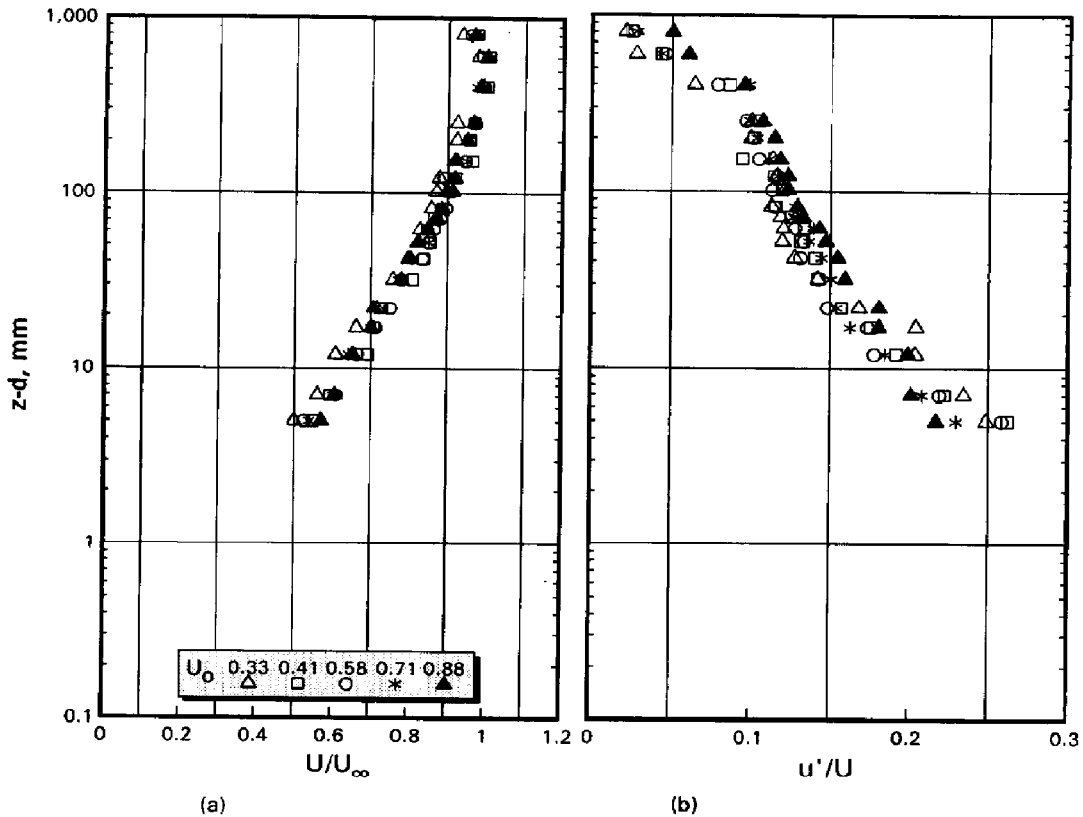


Fig. 2. Characteristics of upstream boundary layer. (a) Mean velocity profiles. (b) Turbulence intensity profiles.

Fig. 2, typical of a neutral atmospheric boundary layer. The roughness length, z_0 , was in the range 0.05–0.15 mm which, at a scale of 1:1000 (based on the wind tunnel boundary layer depth of about 0.6 m and a typical full scale value of about 600 m), corresponds to a rural terrain with $z_0 = 5\text{--}15$ cm.

Low wind speeds were necessary for many of the experiments, although not as low as in some of the pooling experiments of BTS since, in the present case, lower Richardson numbers were generally required. Most experiments were undertaken at four ambient wind-tunnel speeds, corresponding to (nominal) U_0 values of 0.33, 0.58, 0.82 and 1.12 m/s. Since it is particularly difficult to measure velocities around 0.5 m/s or lower, uncertainties in the lowest reference velocity may be as high as $\pm 10\%$. As in the earlier experiments of BTS, the reference velocity, U_0 , was taken throughout as the value at $z = H/4$, on the basis that this is more representative of the velocity field near the top of the valley and that in the recirculating flow within the valley than is the free-stream velocity.

The source-gas mixture was introduced into the valley through a perforated tube, laid spanwise along the valley floor. Source-gas flow rates were always sufficiently small to imply a negligible effect on the flow field within the valley. Even the maximum value of V_s , around 60,000 cm^3/min , implies a local injection

velocity over the 4 cm by 200 cm region just above the pipe of less than $0.04U_0$. In the transient experiments, a vacuum pump was switched into the line simultaneously with the supply being removed. A small volume of gas was thus removed from the valley but this procedure ensured that no further gas leaked into the valley. Mixtures of carbon dioxide (CO_2) and propane (C_3H_8) were used as the source in the heavy gas experiments. The propane was included as a tracer, with concentrations determined by drawing ambient samples through a rake of sampling tubes (2.4 mm o.d.) and passing these samples through hydrocarbon measurement systems (Beckman, model 400 flame ionisation detectors — FID's). The system response time was about one second, which was small enough to be acceptable even in the transient experiments, where typical valley 'flushing' times exceeded 20 seconds. For the neutral release experiments ethane (C_2H_6) was used as the tracer. The analysers have a linear response over a very wide dynamic range and were frequently calibrated with air and a 0.9% ethane mixture. Flow rates of each gas were measured and monitored using Meriam laminar flow elements, with a Brooks flow calibrator used to determine the set points for given pressure drops across them. In the transient runs the 'zero' points of the FID's were reset at the background concentration in the tunnel, which was measured frequently. Measured concentrations in all propane experiments were multiplied by a calibration factor of 0.745 (since ethane was used for analyser calibrations).

The output from each FID was digitised at typically 1–10 Hz and collected by a personal computer. Sampling durations were typically two minutes in the steady-state cases and up to about four minutes in the transient cases. Concentration measurements were generally found to be repeatable to within $\pm 5\%$.

In most experiments concentrations were measured simultaneously at five points within the valley, with sampling tubes mounted either on the three-directional traverse gear in the tunnel or through holes in the valley surface. It was found, not surprisingly, that the largest concentrations invariably occurred near the upwind wall of the valley; this location is deep within the separated flow region and consequently, when the source is removed, it is in this region that the concentration falls most slowly. In the transient experiments, the concentration was therefore measured at five points distributed on the valley upwind surface along a spanwise line about halfway up the valley. With the coordinate system shown in Fig. 1, the five points were at y -positions of 0, ± 0.35 and ± 0.74 (normalised by the valley half-length, $L/2$). In view of the large variability in any single realisation of concentration vs. time, the procedure employed by Hunt and Castro [3] was used. Each transient experiment was repeated 10–20 times, with the concentration at every measurement point then being ensemble-averaged. Figure 3 presents a typical result; variations of $C(t)/C_0$ are shown for each of the five sample locations, with $t=0$ being the time at which the source gas is shut off. Notice that the behaviour is largely independent of spanwise location and that after about 80 seconds, by which time the concentrations have fallen to 10% of their initial values, the

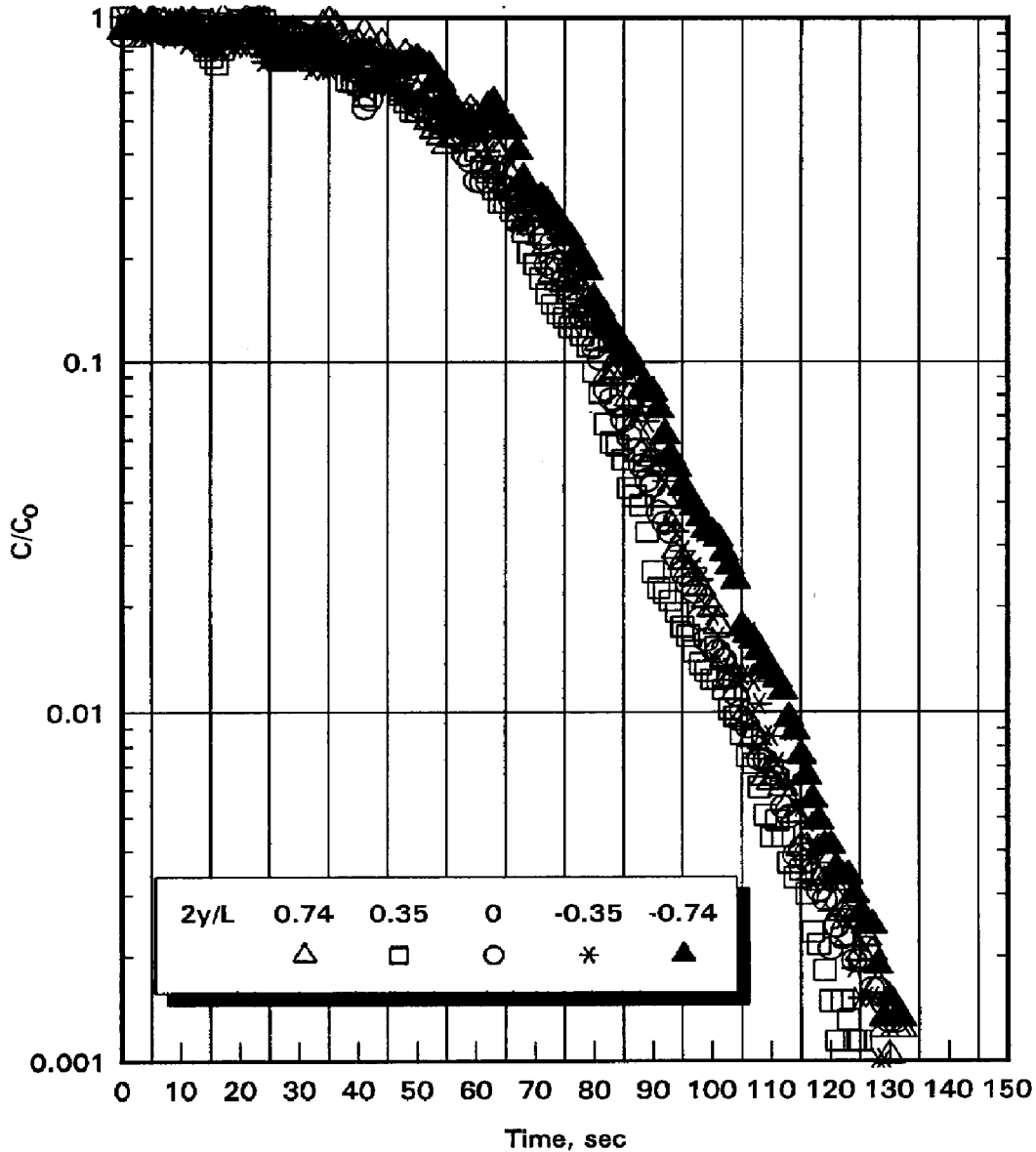


Fig. 3. Concentration decay of heavy gas at different spanwise locations in the large valley. $x = -380$ mm, $z = -105$ mm, $Ri_s = 11.9$.

fall-off in concentration is essentially exponential, as expected on the basis of the ideas discussed in Section 2 (e.g., eq. 9). In all the transient results presented later, data from these five spanwise points were averaged together to reduce the variability even further and, on the basis that three-dimensional effects were not significant, in determining the transient behaviour.

4. Experimental results and discussion

4.1 Pooling limits

Since the primary aim of the work was to study cases in which pooling did not occur, we began by determining, for a typical range of input source rates, the critical tunnel velocity at which pooling just began. Here, pooling is defined as the condition wherein heavy gas within the valley effectively decouples from the wind aloft, so that the heavy-gas concentration at the bottom of the valley equals the source concentration. As explained earlier, entrainment is thereafter (at lower tunnel speeds for the fixed source rate) limited by the processes at the interface between the dense gas pool and the flow above.

Sampling tubes were positioned both inside the source tube and just above it and the steady-state ratios of the two measured concentrations were obtained for fixed source flow rates and gradually increasing tunnel speed. The results are shown in Fig. 4. Figure 5a shows the resulting critical velocity, U_{0c} , taken as the velocity at which the concentration ratio is 0.95, as a function of V_s , the

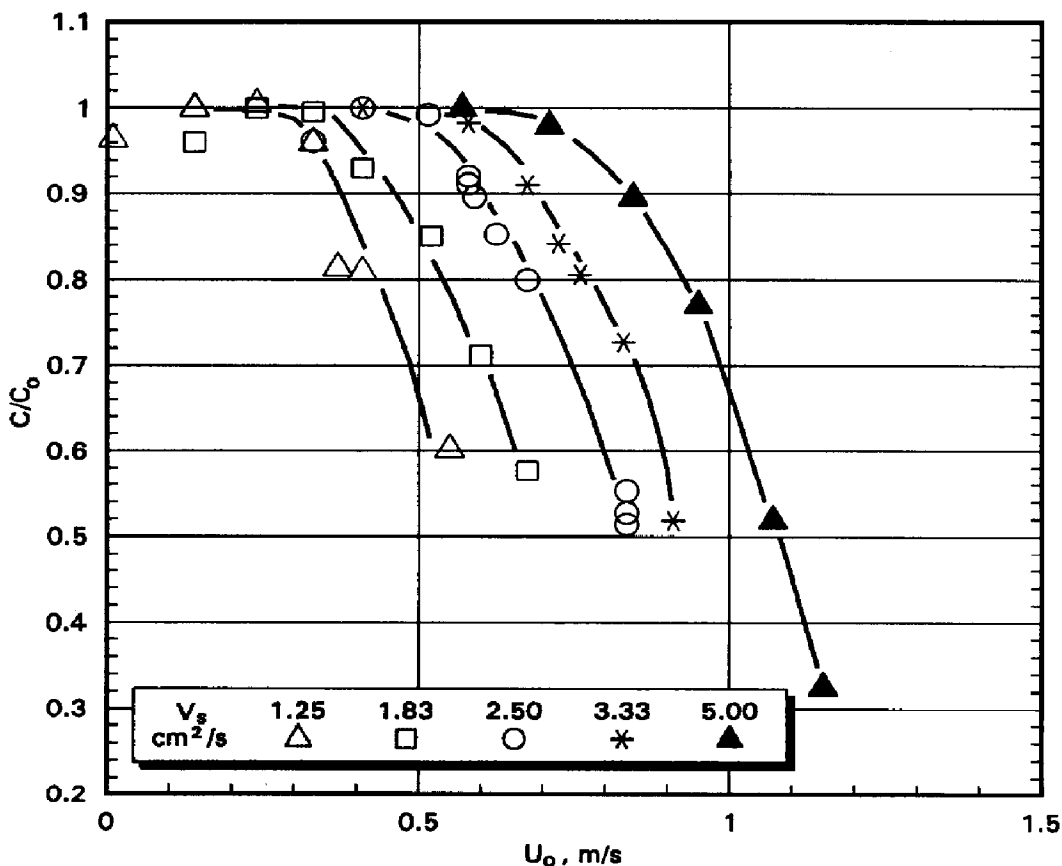


Fig. 4. Pooling condition in the large valley. Pooling begins when C/C_0 reaches 0.95 as U_0 falls.

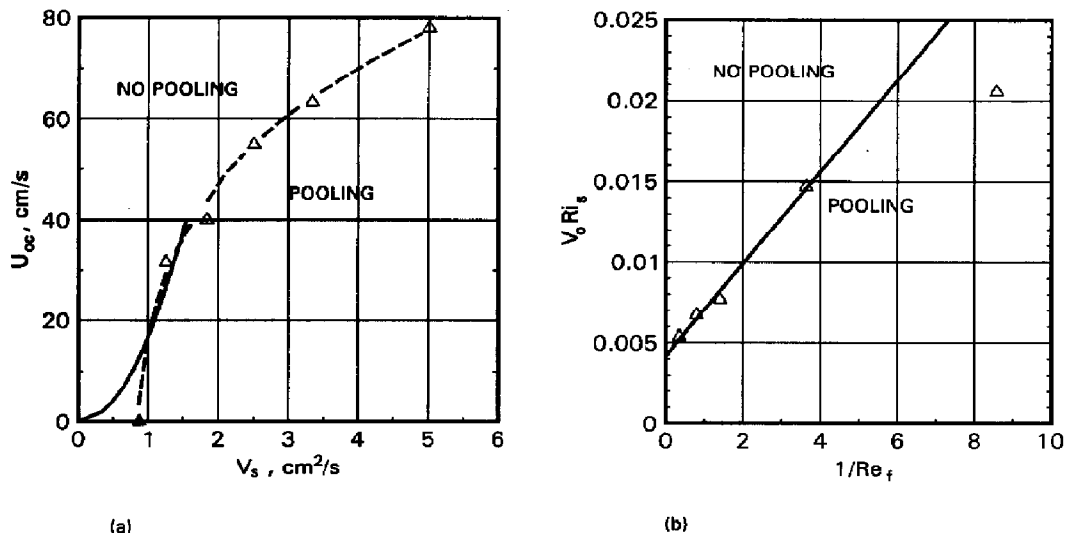


Fig. 5. Critical velocity for pooling conditions. (a) Dimensional plot. (\blacktriangle) is from eq. (13). Solid line is low Re_f limit (eq. 14). (b) Non-dimensional plot. Solid line is eq. (14).

source flow rate. These results are replotted in Fig. 5b as $V_0 Ri_s$ vs. $1/Re_f$ and it is evident that, apart from the lowest Re_f result, the pooling condition satisfies the form of eq. (12) quite well, that is,

$$V' = V_0 Ri_s = 0.0042(1 + 0.68/Re_f). \quad (14)$$

Note that although the constant 0.68 is not too far from the BTS value of 0.46, the other constant is larger by a factor of around nine. However, the arguments leading to eq. (12) were developed for cases in which the pool height, z_p , was large enough to ensure an interface fetch sufficiently long that entrainment was limited by the heaviness of the entrained fluid. The BTS work did not cover cases for which $z_p < 0.2H$ and the constant, c , in eq. (12) was obtained by extrapolating a curve of z_p vs. $V^{1/3}$ to the case of zero pool height, giving $V^{1/3} = 0.08$ for $z_p = 0$. As noted earlier, this is an extrapolation beyond the valid limits of the BTS result. The present data imply $V^{1/3} = 0.16$, which is a factor of two higher than the BTS result; it should be emphasised that the physical processes determining when pooling begins ($z_p = 0$) may well be different from those describing the entrainment process for $z_p > 0.2$. None the less, one expects the pooling limit (V_0) to be a function only of Ri_s and Re_0 , which is certainly confirmed by our data.

Note also that the low Re_f limit of eq. (14) can be expressed as $V_s^2 = 0.0029 W U_0 v$; this is included in Fig. 5a but, although it has the physically correct form for situations in which the entrainment is dominated by molecular processes (i.e. $Re_f \ll 1$, as discussed in BTS), it clearly is not correct for U_0 near zero. In that case, using $\kappa = 0.159 \text{ cm}^2/\text{s}$ (for CO_2 in air), eq. (13) gives a pooling flow rate of about $V_s = 0.875 \text{ cm}^2/\text{s}$ for the large valley. This result is

also included in Fig. 5a and is not inconsistent with an extrapolation of the data for small U_0 .

4.2 Neutral releases

An initial series of experiments was undertaken in both valleys using ethane. Steady-state conditions were set up first and average concentrations (from the five sampling points, as discussed in Section 3) were obtained, before removing the source and obtaining concentrations as a function of time. Figure 6 shows C_0 , the steady-state concentration, plotted against V_0 . In the absence of Reynolds number effects one would expect a linear relationship, with a slope which would depend on the valley slopes and on the particular locations of the sample tubes. It is seen that the results are a reasonable fit to straight lines except those obtained at the lowest tunnel speed (U_0 values in brackets), which lie somewhat lower. Since the results are ensemble averages of very many measurements, these two points cannot be explained away on the basis of statistical scatter and we must conclude that Reynolds number effects were not entirely negligible at these very low tunnel velocities. Molecular diffusion is expected to make a significant contribution to the total dispersion, so one might expect a lower concentration at a given V_0 ; this is in line with the result in Fig. 6. The data suggest that ε (in eq. (10), with $Ri_0=0$ for neutral releases) has the value 16.7 for the large valley, if the lowest Reynolds number result is ignored. This latter data point implies the rather lower value of $\varepsilon=11.8$. Corresponding values for the small valley are some 30% higher; this must be due to the geometrical differences between the valleys (the small valley was proportionately deeper than the large one) and/or the differences in parameters like z_0/H and δ/H . We would expect increases in the latter parameters to cause a reduction in the valley concentration, which is the reverse of what the data indicate, so conclude that geometrical effects were probably dominant. These may have included small differences in the relative locations of the sampling tubes in the two cases.

Figure 7 shows the results of the corresponding transient runs for the large valley case. Concentrations have been normalised by the appropriate C_0 values and in each case it is clear that after an initial delay the decay rate is closely exponential. Denoting t_d as the time required for a fall in $C(t)$ of a factor of ten in this exponential region, Fig. 8a shows $1/t_d$ as a function of U_0 ; we again expect this to be linear in the absence of Reynolds number effects. At the lowest tunnel speeds the large valley results appear to deviate a little from linearity — this deviation might be expected, since even if one could force $U_0=0$ as soon as the source gas were removed, the ethane would gradually disperse via molecular diffusion, so that $1/t_d$ must remain non-zero for $U_0=0$. However, the small valley data do not show the same deviations. Figure 8b shows a plot of the dimensionless time constant, $\tau = U_0 t_d / [H \cdot \ln(10)]$, against Reynolds number, $U_0 H / \nu$. (t_d is the time for a one-decade fall in concentration.) The plot includes data from the transient dense gas releases in the large valley, obtained by fitting straight lines through the low concentration regions

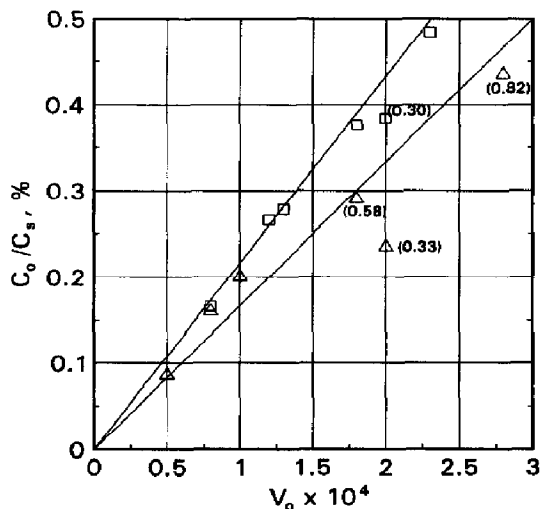


Fig. 6. Steady-state concentration versus source rate for neutral releases. (Δ) large valley, and (\square) small valley. U_0 values shown in parentheses (m/s).

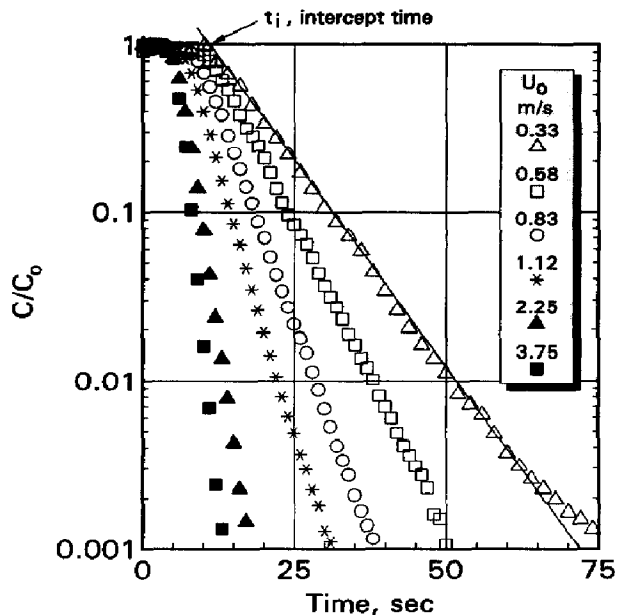


Fig. 7. Concentration decay for neutral releases at various U_0 . (Large valley data.)

($C/C_0 \ll 1$), where the gas behaves as a passive release. A Reynolds number effect in the case of the large valley is only marginally evident above the scatter. The data suggest an average decay time constant, τ , of about 14.5.

These data (Figs. 6 and 8) are generally consistent with the theoretical arguments outlined in Section 2. Note that there is some inevitable uncertainty about when $C(t)$ first begins to fall. The gas samples take a few seconds to travel down the tubes to the FID's and, further, the concentration at the sample positions will not instantaneously follow those just above the source. Figure 9 shows the intercept time, t_i (see Fig. 7), as a function of $1/U_0$. The data are rather scattered, particularly in the large valley case, but are consistent with a 'sampling tube travel time', t_1 , (i.e. t_i at $1/U_0 = 0$) of about 4.8 seconds. Provided the vacuum pumps drawing the samples through the system are reasonably stable, this travel time should be largely independent of any other experimental conditions. The distance between the source and the sampling position, divided by the (linear) slope through the data points in Fig. 9, is equivalent to a normalised 'advection' velocity, U_a/U_0 ; the results suggest $U_a/U_0 = 0.14$ and 0.41 in the large and small valley cases, respectively. These seem to be reasonable results but it should be emphasised that the advection velocity should more properly be thought of as a turbulent transport velocity, since the sampling position is on the surface, deep inside the recirculating region, where actual mean velocities are very low. (At the surface, of course, they are zero.) Note that the larger value (0.41) found for the small valley is

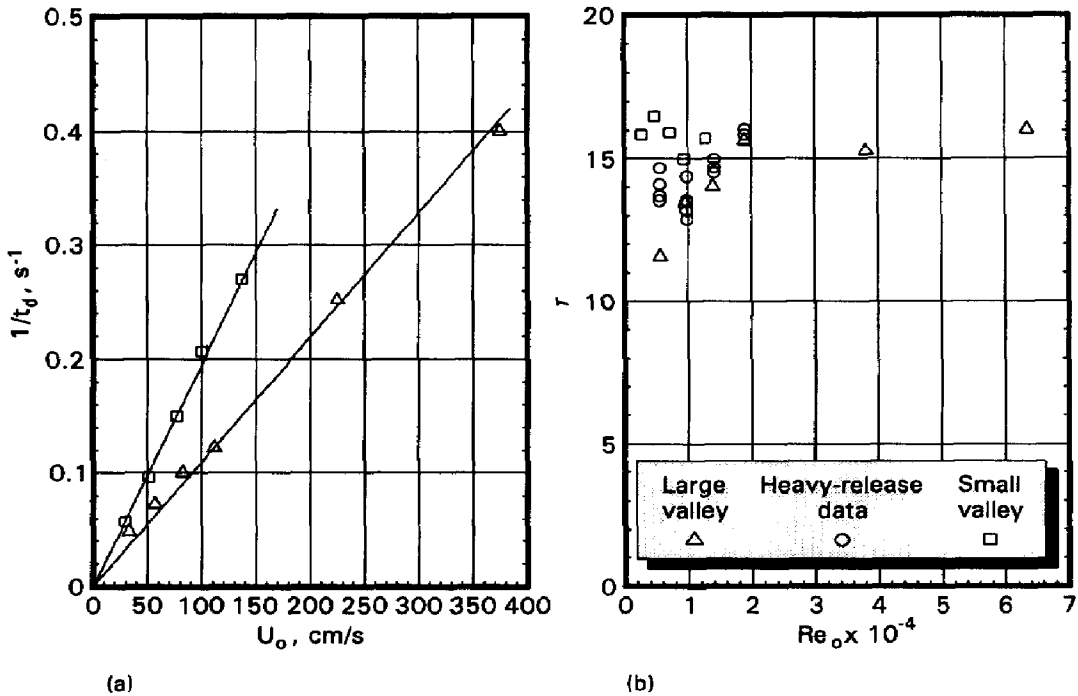


Fig. 8. Time constants of concentration decay for neutral releases. (a) One-decade decay time versus U_0 . (b) Normalised time constant versus Re_0 .

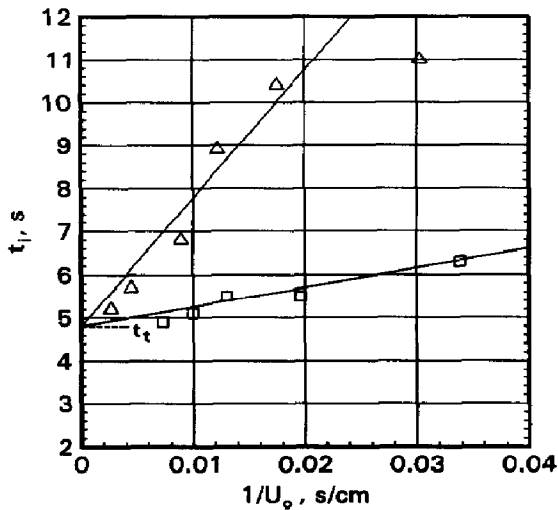


Fig. 9. Intercept time for neutral releases in: (Δ) large, and (\square) small valleys.

qualitatively consistent with the larger z_0/H for this case, although the difference seems rather greater than can be accounted for by the relatively stronger turbulence effects. Again, geometrical differences are probably not insignificant.

4.3 Heavy gas releases

Releases of carbon dioxide and propane mixtures were made in the large valley with various flow rates at four different tunnel speeds, corresponding to $U_0 = 0.33, 0.58, 0.82$ and 1.12 m/s. Values of the governing variables (U_0 and V_0) and corresponding non-dimensional parameters (Re_0 , Ri_s , Ri_0 and V_0) are given in Table 2, along with the principal results for both the steady-state averaged concentration at the sampling locations (C_0 and hence Ri_0) and the intercept time, t_i (and hence t'_i). The latter was deduced from the transient experiments by drawing a straight line through the $C' \ll 1$ region of the semi-log plots of $C'(t)$ vs. t , with a slope corresponding to the averaged decay time from Fig. 8b (14.5, as discussed in the previous section). A typical set of the transient results for fixed U_0 (0.58 m/s) is shown in Fig. 10. It is clear that as the flow rate increases, so that steady-state concentrations become larger, the initial decay is delayed, as expected. Eventually, however, the decay rate becomes identical with that of a neutral release at the same U_0 , as expected.

It should be emphasised that the time dependence of the concentration was found not to be a strong function of the sampling location. This is demonstrated in Fig. 11, which shows a set of results for a particular, but typical, case ($U_0 = 0.58$ m/s, $Ri_s = 3.85$, $V_0 = 0.000565$). The sampling location corresponding to each curve is shown on the inset diagram and it is evident that only for the locations closer than about $0.2 H$ to the source does the measured concentration start to decay noticeably earlier than elsewhere. All sampling locations were within, or very close to, the mean separation region, except for one port just beyond the downstream edge of the valley. At this location the decay is delayed rather longer, as would be expected.

In accordance with eq. (10), the steady-state values of C_0 are plotted in Fig. 12 in the form $(C_0/(C_s \varepsilon V_0) - 1)$ vs. Ri_0 , with the ε value implied from the earlier neutral release experiments (16.7 for the large valley, see previous section). It can be seen that data obtained at the lowest U_0 generally lie a little below the rest of the data, which is, again, almost certainly a Reynolds number effect. If the ε value for those particular points is adjusted to the value (11.8) implied by the $U_0 = 0.33$ m/s data point on Fig. 6, agreement is noticeably improved. The corrected points are included in Fig. 12 and most data cluster quite well around a straight line whose slope (n , in eq. 10) is about 0.5. (The exceptions are largely for cases in which the propane flow rates are at their lowest so that possible measurement inaccuracies are greatest.) These results would seem to provide reasonable confirmation of the assumed form of the entrainment relation (eq. 7).

Equation (11) implies that the intercept time, t'_i , defined earlier, should satisfy the relation:

$$t'_i/\tau = (\alpha/n) Ri_0^n. \quad (15)$$

In Fig. 13 t'_i/τ is plotted against Ri_0 and a line of slope $n = 0.5$ (deduced earlier from the steady-state data, Fig. 12) is included in the figure. The sampling tube travel time (4.8 s), deduced from the neutral data (Fig. 9), has been subtracted

TABLE 2

Principal variables for heavy gas experiments

U_0 (m/s)	Re_0 ($U_0 H/\nu$)	Ri_s [$gH\Delta\rho_s/(\rho_a U_0^2)$]	V_s (cm^2/s)	C_0/C_s (%)	Ri_0 ($Ri_s \cdot C_0/C_s$)	$V_0 \times 10^4$ ($V_s/U_0 H$)	$(t_1 - t_0)$ (s)	t'_1 [$U_0(t_1 - t_0)/H$]
0.33	5588	11.9	0.152	0.330	0.0390	1.813	14.5	18.84
0.33	5588	11.9	0.425	1.870	0.2230	5.070	51.1	66.39
0.33	5588	11.9	0.667	3.510	0.4180	7.957	93.1	121.0
0.33	5588	11.9	0.917	5.410	0.6440	10.94	120.1	156.0
0.33	5588	11.9	1.167	6.900	0.8210	13.92	150.2	195.1
0.58	9821	3.85	0.125	0.198	0.0076	0.848	9.10	20.78
0.58	9821	3.85	0.833	2.200	0.0847	5.654	26.9	61.43
0.58	9821	3.85	1.500	4.270	0.1640	10.18	45.1	103.0
0.58	9821	3.85	2.125	6.760	0.2600	14.42	61.1	139.5
0.82	13885	1.93	0.083	0.092	0.00177	0.399	3.70	11.94
0.82	13885	1.93	0.250	0.252	0.00486	1.200	6.00	19.37
0.82	13885	1.93	0.833	1.070	0.0207	3.999	9.00	29.06
0.82	13885	1.93	1.667	2.290	0.0442	8.004	14.0	45.20
0.82	13885	1.93	2.500	3.120	0.0602	12.00	20.3	65.54
0.82	13885	1.93	3.500	6.500	0.1250	16.80	27.7	89.43
0.82	13885	1.93	4.500	8.110	0.1570	21.61	30.7	99.11
1.12	18965	1.033	2.208	3.120	0.0400	7.762	6.10	26.90
1.12	18965	1.033	4.458	5.870	0.0620	15.67	9.70	42.77

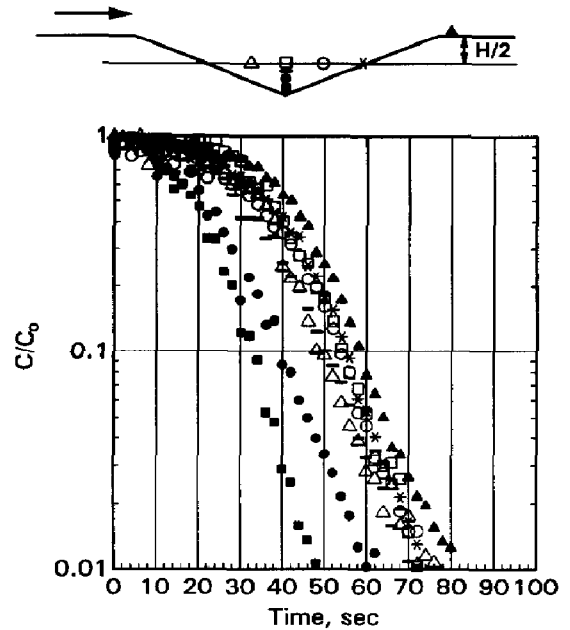
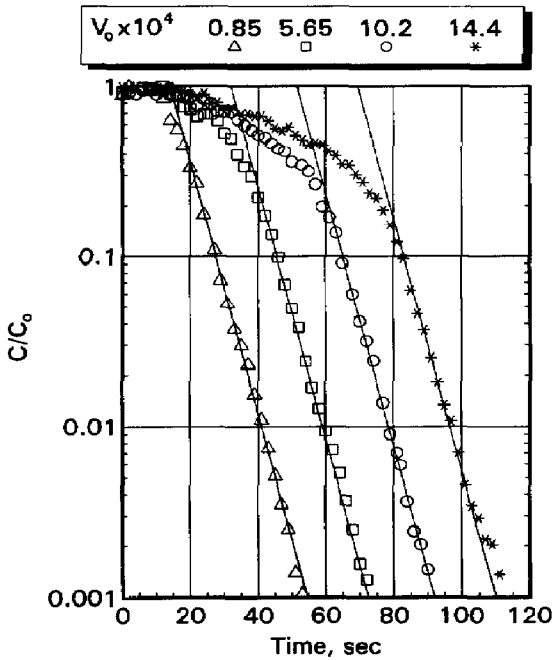


Fig. 10. Concentration decay for heavy gas releases. U_0 fixed at 0.58 m/s. Solid lines have slope measured for neutral release at same U_0 .

Fig. 11. Concentration decay for heavy-gas releases at different points in the valley. ($U_0=58$ cm/s, and $V_s=0.83$ cm³/s.)

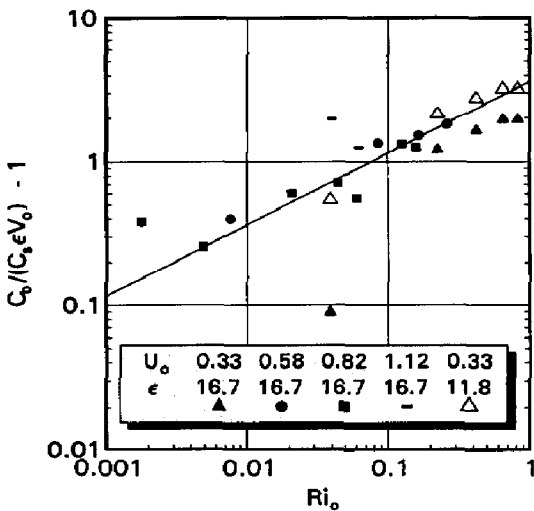


Fig. 12. Data fit to eq. (10). Line has slope of 1/2.

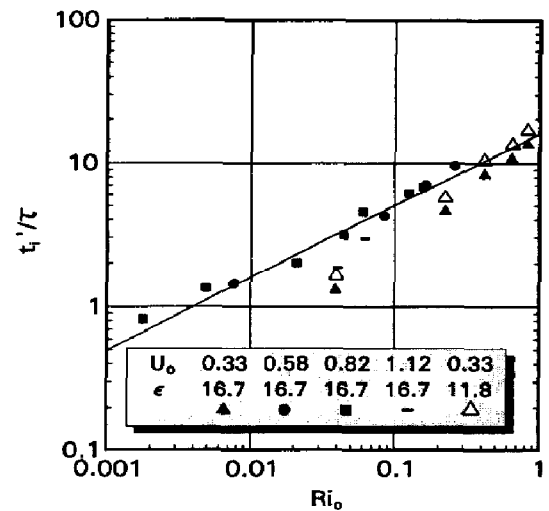


Fig. 13. Normalised intercept time as a function of Ri_0 (eq. 15). Line has slope of 1/2.

from the measured t_i . Again the data seem to be reasonably consistent with the expected form. Note that in this plot the average τ value (14.5) has been used as before, but data using $\tau = 11.6$ ($\varepsilon = 11.8$) for the lowest Reynolds number set is included; this improves the collapse somewhat. However, if an effective ‘advection’ time, accounting for the delay between $t = 4.8$ s (the tube travel time) and when the concentration at the sampling position begins to fall, is subtracted from the measured t_i data the results for the lowest U_0 case in Fig. 13 would again fall somewhat below the values shown. In fact, one might expect such an advection delay to increase somewhat for the larger values of Ri_s . We have made no attempt to account for this in comparisons with our theory since it would be inconsistent to do so without at the same time allowing some of the ‘constants’ used in the theory also to be functions of Ri .

5. Final discussion and application

We restate the major conclusions reached on the basis of the simple theoretical ideas discussed in Section 2. These are that the steady-state concentration in the valley satisfies

$$C_0/C_s = \varepsilon V_0(1 + \alpha Ri_0^n), \quad (10)$$

where $Ri_0 = C_0/C_s Ri_s$, $V_0 = V_s/U_0H$ and α and ε are constants. If the source is removed, the concentration within the valley (inside the separated region) decays like

$$-\ln(C') + \alpha Ri_0^n(1 - C'^n)/n = t'/\tau, \quad (11)$$

where $C' = C(t)/C_s$ and τ is a decay time-constant. Our experimental data (for neutral releases and for heavy-gas releases after the initial effects of Ri have decayed) suggest that τ is about 15. Fackrell [8] found that for a rectangular building of breadth b and height h the decay time for dispersion of a release within the separated wake varied like

$$\tau = 11(b/h)^{1.5} / [1 + 0.6(b/h)^{1.5}]. \quad (16)$$

For the large valley, using L/H as the equivalent to b/h , this expression yields $\tau = 17$, which is not much greater than our measured values. Making some allowance for the fact that the separation region behind the building (with that b/h) is somewhat larger than the valley volume, there is encouraging agreement between these results. It seems that the relationship between ‘residence time’ and the separated region volume is close to that found by Fackrell (and by Hunt and Castro [3]) and is, therefore, dominated by turbulent dispersion rather than any mean flow features, as concluded in those earlier works. There is little reason to suppose that this result could not be extended to long valleys of other shapes, provided sensible estimates of the size of the recirculation region could be made.

Our data also follow the forms of eqs. (10) and (11) quite well, with $n=0.5$ and $\varepsilon=16.7$ (except at the lowest Reynolds number, where $\varepsilon=11.8$ provides a better fit). In view of the various assumptions made this might seem rather surprising. Note, however, that the value of α differs by a factor of about two, depending on whether Fig. 12 (for the steady state result, eq. 10) or Fig. 13 (for the transient result, eq. 15) is used to deduce it. In the former case $\alpha=3.7$ and in the latter, $\alpha=7.9$. In this respect our data are *not* wholly consistent with the theory. It should be noted, however, that the α value from data fitted to eq. (10) will depend, to some extent, on the particular sample location used to obtain C_0 . Although we chose a location within the recirculating, well-mixed region, use of a spatially averaged C_0 (over the whole of the separated flow) might yield closer agreement with the α obtained from eq. (15). Nonetheless, there are a number of assumptions inherent in the theory. The most dubious is probably that δ , the thickness of the mixing region, is not a function of Ri (and hence also not a function of time). We assumed $\alpha=k_5(\delta/H)^n=\text{constant}$. Figure 14 shows concentration contours in three cases — one for a neutral release (Fig. 14a), one for a typical dense gas release (Fig. 14b) and one for a dense gas release in which pooling is near occurring (Fig. 14c). It is clear that the nature of the flow is changed substantially in the pooling case, for which the mixing

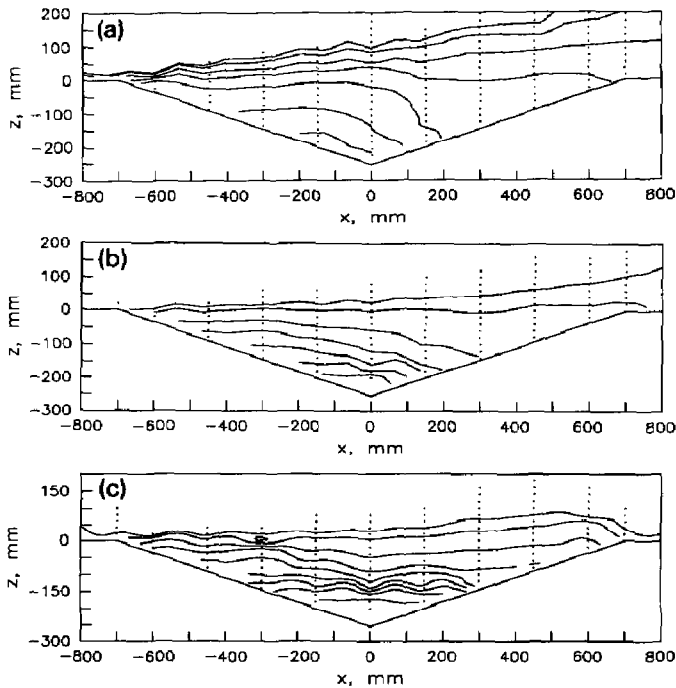


Fig. 14. Steady-state concentration contours (C/C_0 in %) in large valley. Dots show locations of measurement points. (a) Neutrally buoyant release, $Ri_s=0$, $V_0=0.345 \times 10^{-4}$, (b) Moderately heavy gas release, $Ri_s=3.85$, $V_0=5.6 \times 10^{-4}$, and (c) Heavy gas release — near pooling conditions, $Ri_s=3.85$, $V_0=14.3 \times 10^{-4}$.

region is essentially horizontal and the range of concentrations across the depth of the valley varies much more than it does for the neutral release. However, there are much weaker changes for the non-pooling heavy gas release; the contours in Fig. 14b have a very similar shape to those in the neutral case (Fig. 14a). Nonetheless one anticipates that α cannot be strictly constant over the entire range of (non-pooling) dense gas conditions.

It is difficult to construct a 'higher-order' theory in which α is allowed to vary with Ri_0 ; to begin with it is not clear what form such a dependence should take, but even if one were inserted the algebra rapidly becomes unwieldy. We believe, rather, that the sensible approach is to accept these limitations and use eqs. (10) and (11) as the basis of estimates of decay times for heavy gas releases, but employ the two different values of α as appropriate — i.e. 3.7 with eq. (10) to deduce Ri_0 and 7.9 with eq. (11) to deduce decay times. This procedure is relatively straightforward because $n = 0.5$, which means that eq. (10) becomes a quadratic in $(C_0/C_s)^{0.5}$. A typical application will suffice as an example.

Assume that 60 tonnes of chlorine are released within an hour (i.e. around 1000 kg/min) over a 400 m span at the bottom of a valley of depth 50 m and width 250 m (similar proportions to the valleys in our experiments). Our pooling condition (eq. 14) then implies that provided the wind speed above the valley exceeds about 3.6 m/s pooling will not occur. If the wind is lighter than this, the BTS work should be used to estimate flushing times. Let us assume that there is a 4 m/s wind. V_0 and Ri_s have values of 7×10^{-5} and 44.4, respectively, and eq. (10) can then be solved, using $\varepsilon = 16.7$ and $\alpha = 3.7$, to give $C_0/C_s = 0.00265$ and $Ri_0 = 0.118$. Use of eq. (11), with $\tau = 15$ (to be conservative) and $\alpha = 7.9$, then yields a time of about 27 min for the concentrations within the valley to decay to 100 ppm. This is still a highly dangerous concentration level¹. Note that each additional decade of decay requires about a further 7 minutes — $(H\tau \ln(10)/U_0)$ — the neutral result. Release of a neutral gas under similar conditions (the same V_s) would lead to about a 10-minute decay to the 100 ppm level, so the heaviness of the chlorine has more than doubled the time required to flush the valley to 100 ppm. The original specification of a one-hour spill was chosen to ensure that effectively steady-state conditions occur before the release is stopped. Shorter releases at the same flow rate would lead to shorter decay times, of course.

6. Acknowledgements

We are grateful to the staff of the Fluid Modeling Facility, US Environmental Protection Agency, for making this research possible. IPC acknowledges the support of EPA Cooperative Agreements CR-814346 & CR-817931,

¹ A referee has pointed out that, of course, the dose (concentration integrated over exposure time) would in this case have been fatal long before the 100 ppm level was reached.

while a Visiting Professor at NC State University, AK is grateful for the advice and encouragement of Dr Gary Briggs and for the support of EPA Cooperative agreement CR-814346 while a graduate student, and SPSA acknowledges support from both these EPA Agreements. This paper has been subjected to EPA review and approved for publication. Mention of trade names or commercial products does not constitute endorsement or recommendation for use.

Notation

A	area across which fluid is entrained out of the valley (L^2)
C_0	average volumetric concentration of gas in valley
C_s	source-gas concentration
C	spatially-averaged, time dependent gas concentration in valley
C'	C/C_0 , dimensionless concentration
F	flux of concentration out of valley (L^3/T)
H	depth of valley (L)
$k_1 - k_5$	non-dimensional constants
L	spanwise length of valley (L)
n	dimensionless exponent (eq. 7)
Re_0	U_0H/ν , Reynolds number
Re_f	$(H/W)V_0Re_0/Ri_s$, modified shear Reynolds number (eq. 12)
Ri	$g(\Delta\rho/\rho_a)\delta/U_0^2$, Richardson number
Ri_0	Ri_sC_0/C_s , steady-state valley Richardson number
Ri_s	$\gamma C_s gH/U_0^2$, source Richardson number
t	time (T)
t'	tU_0/H , dimensionless time
t_d	time for one-decade decay in concentration (T)
t_i	intercept time, i.e. time at $C' = 1$ on linear extrapolation of exponential decay region (see Fig. 7) (T)
t_r	travel time of sample within tube leading to analyzer (T)
$U(z)$	ambient approach velocity (L/T)
U_e	entrainment velocity (L/T)
U_0	approach flow velocity at $z = H/4$ (L/T)
V	volume of valley (L^3)
V_s	volumetric flow rate of source gas, per unit cross-stream length (L^2/T)
V_0	V_s/HU_0 , dimensionless source flow rate
V'	V_0Ri_s
W	width of valley in flow direction (L)
W'	surface area (per unit width) of top of diffusing layer above heavy-gas pool (L)
x, y, z	Cartesian coordinates (axial, spanwise and vertical directions, respectively)
z_0	roughness length (L)

Greek

α	$k_5(\delta/H)^n$, dimensionless constant, (eq. 10)
γ	$(\Delta\rho_s/\rho_a)C_s$, factor relating concentration to density difference
δ	average entrainment layer thickness (L)
ε	$1/(k_1k_2k_3)$, dimensionless coefficient (eq. 10)
κ	molecular diffusivity (L^2/T)
ν	kinematic viscosity (L^2/T)
ρ_a	ambient air density (M/L^3)
ρ_s	source gas density (M/L^3)
$\Delta\rho_s$	density difference between source gas and ambient air (M/L^3)
θ	angle of valley side-wall slope
τ	$k_4/(k_1k_3)$ (eq. 11) = $U_0t_d/[H\ln(10)]$ (Fig. 8b), dimensionless decay time constant

References

- 1 G.A. Briggs, R.S. Thompson and W.H. Snyder, Dense gas removal from a valley by crosswinds, *J. Hazardous Mater.*, 24 (1990) 1–38.
- 2 G.C. Christodoulou, Interfacial mixing in stratified flows, *J. Hydraulic Res.*, 24 (1986) 77–92.
- 3 A. Hunt and I.P. Castro, Scalar dispersion in model building wakes, *J. Wind Eng. Ind. Aerodyn.*, 17 (1984) 89–115.
- 4 J.A. Peterka and J.E. Cermak, Turbulence in building wakes, 4th Int. Conf. on Wind Effects on Buildings and Structures, London, Sept. 8–12th, 1975.
- 5 I.P. Castro and W.H. Snyder, A wind tunnel study of dispersion from sources downwind of three-dimensional hills, *Atmos. Environ.*, 16 (1982) 1869–1887.
- 6 W. Humphries and J.H. Vincent, Experiments to investigate the transport processes in the near wake of discs in turbulent airflow, *J. Fluid Mech.*, 75 (1976) 737–749.
- 7 J.H. Vincent, Scalar transport in the near aerodynamic wakes of surface-mounted cubes, *Atmos. Environ.*, 12 (1978) 1319–1322.
- 8 J.E. Fackrell, Parameters characterising dispersion in the near wake of buildings, *J. Wind Eng. Ind. Aerodyn.*, 16 (1984) 97–118.
- 9 W.H. Snyder, The EPA Meteorological Wind Tunnel: Its design, construction and operating characteristics, Report No. EPA-600/4-79-051. U.S. Environmental Protection Agency, Research Triangle Park, NC, 1979, 78 pp.